



# Dendritic spine dynamics in synaptogenesis after repeated LTP inductions: Dependence on pre-existing spine density

Yuki Oe\*, Keiko Tominaga-Yoshino, Sho Hasegawa & Akihiko Ogura

Department of Neuroscience, Osaka University Graduate School of Frontier Biosciences, Yamadaoka 1-3, Suita 565-0871 Osaka, Japan.

Not only from our daily experience but from learning experiments in animals, we know that the establishment of long-lasting memory requires repeated practice. However, cellular backgrounds underlying this repetition-dependent consolidation of memory remain largely unclear. We reported previously using organotypic slice cultures of rodent hippocampus that the repeated inductions of LTP (long-term potentiation) lead to a slowly developing long-lasting synaptic enhancement accompanied by synaptogenesis distinct from LTP itself, and proposed this phenomenon as a model system suitable for the analysis of the repetition-dependent consolidation of memory. Here we examined the dynamics of individual dendritic spines after repeated LTP-inductions and found the existence of two phases in the spines' stochastic behavior that eventually lead to the increase in spine density. This spine dynamics occurred preferentially in the dendritic segments having low pre-existing spine density. Our results may provide clues for understanding the cellular bases underlying the repetition-dependent consolidation of memory.

From our daily experience, we know that the repetition of practice is almost always required for the establishment of long-lasting memory. In more systematic behavior biological analyses, this is true. At the dawn of modern memory research, Ebbinghaus showed that repeated task performance decelerated the “forgetting curve” for a random list of meaningless words<sup>1</sup>. Pavlov presented a conditioning stimulus repeatedly to his dogs before establishing an association with an unconditioned stimulus<sup>2</sup>. This effect exists in invertebrates too, as repeated sensitisation of the *Aplysia*'s gill withdrawal reflex prolongs the retention of memory<sup>3</sup>. In recent studies, it is reported that some molecules are also required to be activated repeatedly for memory consolidation: repeated activations of cAMP-MAPK signaling coupled with circadian rhythm are indicated to be necessary for memory consolidation *in vivo*<sup>4–6</sup>. To reveal the cellular mechanisms underlying this repetition-dependent consolidation of memory, an appropriate *in vitro* model is required, as LTP (Long-Term Potentiation) in acutely isolated hippocampus is powerful for unveiling cellular and molecular mechanisms underlying memory trace formation<sup>7,8</sup>.

We previously found in the stable organotypic slice cultures of the rat hippocampus<sup>9</sup> that the enhancement of synaptic strength by a single induction of LTP by chemical means disappeared within 24 h but that three repeated LTP inductions with 3–24 h intervals lead to another phase of synaptic enhancement which develops slowly (after the disappearance of effect of the third LTP) and lasts for more than 3 weeks<sup>10,11</sup>. This synaptic enhancement is independent of cell survival but is accompanied by the formation of new synapses<sup>10–12</sup> requires protein synthesis<sup>13</sup>, and is specific to the stimulated input pathway<sup>14</sup>. Electrical tetanization can replace chemical induction of LTP<sup>14</sup>. We name this novel long-lasting structural plasticity phenomenon RISE (Repetitive-LTP-Induced Synaptic Enhancement), and propose it as an *in vitro* model system for analyzing the cellular bases of the repetition-dependent consolidation of memory.

Here we examine the dynamics of each dendritic spine following RISE-producing stimulation in a time-sequenced manner, using slice cultures prepared from transgenic mice having fluorescence-labelled CA1 pyramidal neurons in their hippocampi. The questions we addressed here are: 1) whether or not the spines grow in number by simply increasing the rate of generation of spines; 2) what is occurring during an apparent latent period between the third LTP induction and the onset of spine number increase; 3) whether or not the spine

SUBJECT AREAS:  
SYNAPTIC PLASTICITY  
LEARNING AND MEMORY  
CELLULAR NEUROSCIENCE  
MOTILITY

Received  
4 April 2013

Accepted  
17 May 2013

Published  
6 June 2013

Correspondence and requests for materials should be addressed to A.O. (oguraa@fbs.osaka-u.ac.jp)

\* Current address:  
RIKEN Brain Science Institute, Hirosawa 2-1, Wako 351-0198 Saitama, Japan.

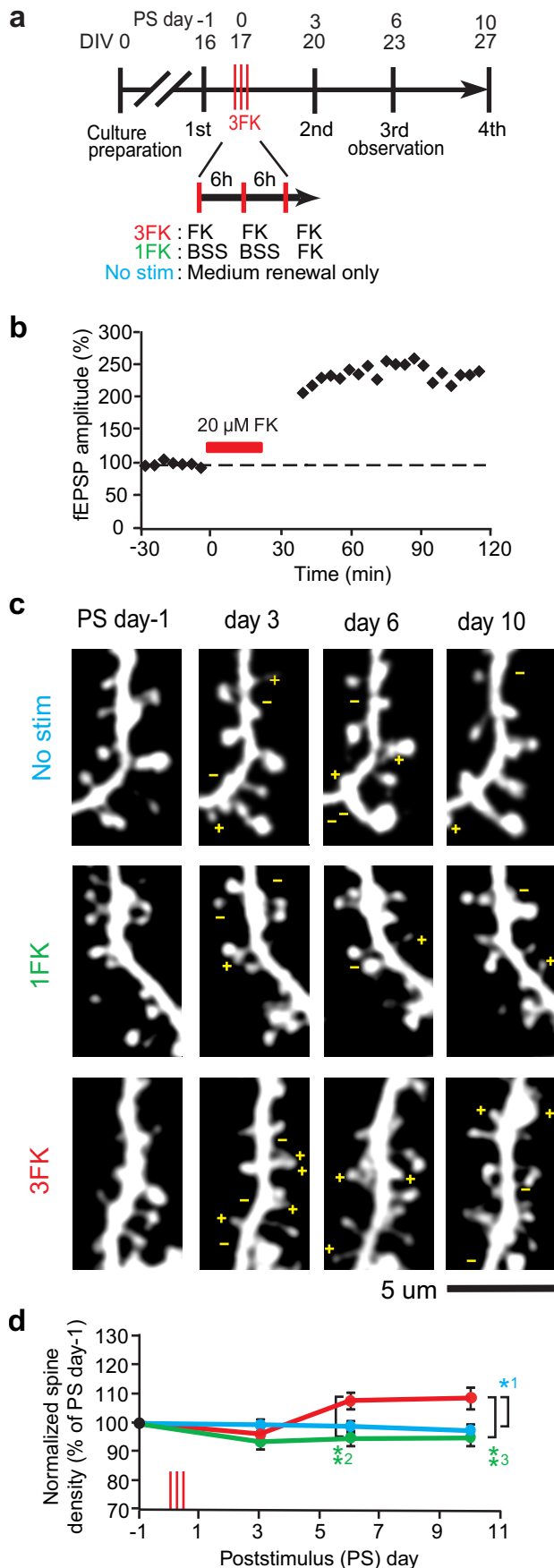


**Figure 1** | Increase in spine density after 3 repeated inductions of chemical LTP in cultured mouse hippocampal slices. (a) Timeline of experimental procedures. The day of 3 LTP inductions (=PS

[poststimulus] day 0) typically corresponds to 17 DIV (days *in vitro*). Images were obtained 4 times at PS days -1, 3, 6 and 10. (b) Chemical inductions of LTP (representative recording). Note that the EPSP amplitude increases without any need of test stimuli. This nature is important, since we delivered no electric pulses for RISE production. (c) Representative time-sequenced images of dendritic segments. Plus and minus symbols in each picture indicate the spines generated and retracted, respectively, as determined by comparing 2 time-consecutive images. (d) Development of RISE after 3 LTP inductions. Note here that 3FK specimens show no net spine density increase at PS day 3. The numbers of dendritic segments examined are 30, 32 and 42, for No stim, 1FK and 3FK specimens, respectively. Statistic comparison was made by 2-way ANOVA followed by Bonferroni's test. *P* values are 0.038 for \*1, 0.0057 for \*\*2 and 0.0098 for \*\*3.

dynamics is uniform irrespectively to the density of pre-existing spines. The first question is related to the fact that the spines are perpetually fluctuating<sup>15</sup>. The second question is related to the fact that there is a considerably long delay before the spine number increase becomes apparent<sup>10–12</sup>. The third question is related to a recently emerging theory of “clustered synaptogenesis” in which synapse formation is regulated not on a basis of individual synapse but on a basis of population of synapses<sup>16–18</sup>. Detailed description of spine dynamics leading to synaptogenesis should provide clues for understanding the subcellular mechanisms that underlie the repetition-dependent consolidation of memory.

## Results

Although there are multiple means for producing RISE<sup>10,11,14</sup>, we chose here the application of forskolin (FK), since there is a report<sup>4</sup> that memory consolidation requires repeated PKA activations *in vivo*. This choice may allow better comparison of the results we obtain here with the previous knowledge. First we confirmed that FK (20 μM, 20 min) induces LTP in the Schaffer collateral-CA1 pyramidal cell synapses in mouse slice cultures as it does in rat slice cultures<sup>8</sup> (Fig. 1a, b). Three repeated inductions of LTP at 6 h intervals was effective to produce RISE in mouse cultures as was the case of rat cultures. Moreover, the time-course of development of RISE, including an apparent delay between the third LTP and the onset of synaptic enhancement, was similar to that of rat cultures (Fig. 1c, d). Single induction of LTP (indicated as “1FK”) or repeated medium renewal (indicated as “No stim”) did not produce RISE-like synaptic enhancement.

Next we estimated the dynamics (generation and retraction) of individual dendritic spines by comparing two consecutive images obtained at regular intervals (Fig. 2). Without any stimulus, spines were generated and retracted continuously as previous reports showed in the cortex<sup>19–21</sup> (Fig. 2a). This stochastic behavior is also consistent with the rat cultures described by Yasumasu *et al.*<sup>15</sup> After repeated LTP inductions, however, a remarkable change in spine dynamics was seen. Even at poststimulus (PS) day 3, when no net change in the spine number was apparent yet, both the rates of generation and retraction of spines increased (Fig. 2c, d). At PS day 6, the rate of retraction returned to its prestimulus level, while that of generation sustained its high value, resulting in a net increase in spine density (Fig. 2c, e). At PS day 10, the rate of generation also returned to its prestimulus level, resulting in equilibrium and therefore constant spine density from then on (Fig. 2c, f). Thus the increase in spine density resulted from a transient collapse in the dynamic equilibrium between spines' generation and retraction. 1FK also showed slight increase of spine dynamics at PS day 3, though it was not significant. The spine dynamics returned to basal level already at PS day 6 (Fig. 2b, e). This led to no net increase of spine density as shown in Fig. 1.



We next examined electrophysiologically whether newly generated spines are coupled with axon terminals to form functional synapses. We monitored miniature excitatory postsynaptic currents (mEPSC), since the frequency of mEPSC should correlate with the number of functional synapses (Fig. 3a, b). At PS day 3, no increase in mEPSC frequency was recognized. At PS day 6, however, a significant increase was seen. This increase was maintained at PS day 10. Hence, it is highly probable that at least a portion of newly generated spines are accompanied by presynaptic terminals to form functional synapses. This guess is supported by a previous observation by Zito *et al.*<sup>22</sup> who showed new spines generated after glutamate application quickly became functional. The mean amplitude of the mEPSC did not show significant differences throughout the period of observation (Fig. 3c).

We noticed that the density of existing spines was not uniform; the spine density varied considerably among cells, among dendrites of a single cell, and even among segments of a single dendrite (Fig. 4a–c).

Therefore we re-examined the increased spine number (density) of the dendritic segment with respect to pre-existing spine density. As the first approach we divided the dendritic segments to high and low pre-existing spine density (HSD and LSD, respectively) populations, setting a boundary at 1.3 spines/ $\mu\text{m}$  dendrite, which approximated the mean spine density. As shown in Fig. 4d and e, the increase in spine density occurred only in the LSD segments (this is also true when the spine dynamics is seen by chasing individual dendritic segments; see Supplementary Fig. S1 on line).

Next we chased the dynamics of individual spines. Spines' fluctuation increased in both the LSD and HSD populations (Fig. 5a, d). However, compared with the LSD segments, the magnitude of fluctuation in the HSD segments was smaller (Fig. 5g) and the following imbalance in the rates of generation and retraction was smaller (Fig. 5h), thus resulting in little net change in the spine density in 3FK as shown in Fig. 4k. No stim and 1FK specimens showed little change in spine density and spine dynamics in either LSD and HSD segments.

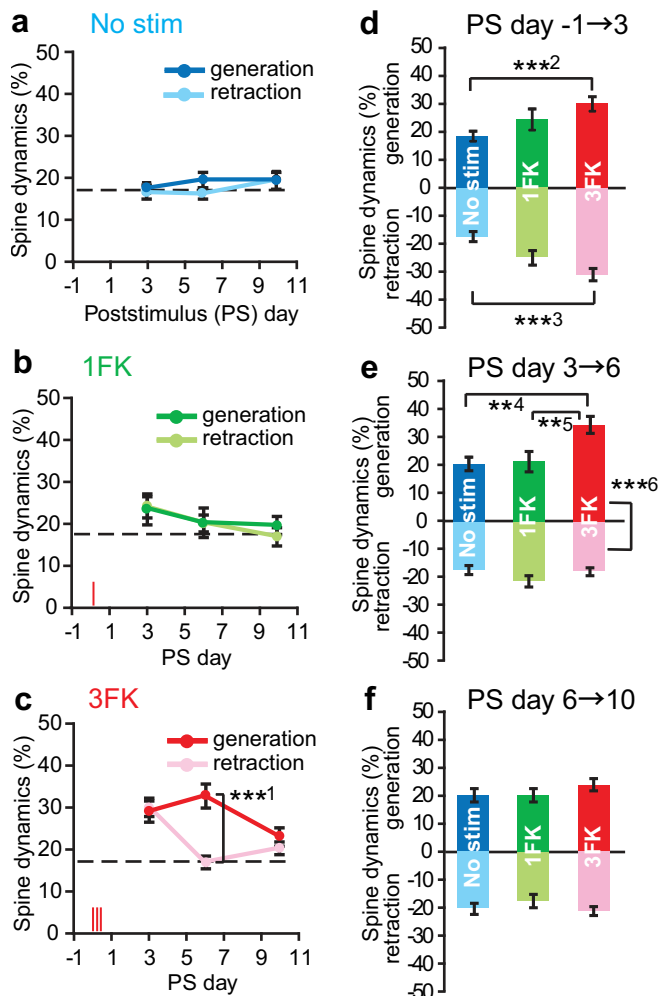


**Figure 2 | Generation and retraction of spines after 3 repeated LTP inductions.** (a–c) Spines generated (deep-coloured) and retracted (light-coloured) as scored by comparisons of 2 time-consecutive images. Broken lines represent the level of constant fluctuation (the value plotted at PS day 3 of No stim specimens). The numbers of dendritic segments examined are 30, 32 and 42, for No stim, 1FK and 3FK specimens, respectively. Statistic comparison was made by paired *t*-test for (a–c) for each time point. *P* value is  $1.3 \times 10^{-5}$  for \*\*\*1 (and \*\*\*6). (d–f) Data re-plotted by matching timings for comparison among varied stimulus conditions. Statistic comparison was made by 2-way ANOVA followed by Bonferroni's test. *P* values are  $7.7 \times 10^{-4}$  for \*\*\*2,  $4.0 \times 10^{-5}$ , for \*\*\*3, 0.0012 for \*\*4 and 0.0021 for \*\*5.

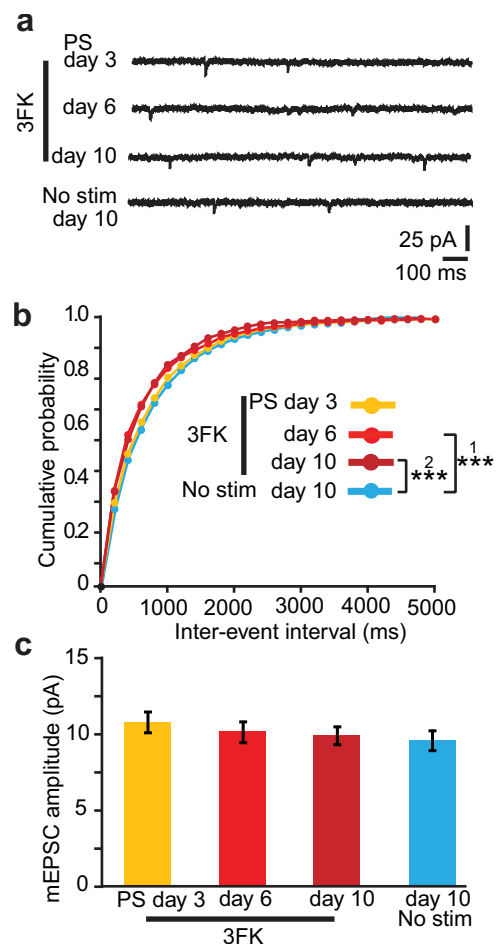


**Figure 3 | Assessment of functionality of new spines.** Increased occurrence of spontaneous miniature EPSC after 3 LTP inductions is shown. (a) Example recordings. (b) Cumulative probability histograms of mEPSC frequency. As plotted with respect to inter-event-interval (delimited by 200 ms bins), a leftward shift of the histogram means more frequent occurrence of mEPSC. The number of neurons examined are 15, 20, 22 and 24, for 3FK PS day 3, 6, 10 and No stim specimens, respectively. Statistic comparison was made by Kormogolov-Smirnov test. *P* values are  $3.1 \times 10^{-9}$  for \*\*\*1 and  $2.7 \times 10^{-8}$  for \*\*\*2. (c) Mean mEPSC amplitudes showing no remarkable changes after 3FK exposures. Sample numbers are the same as in (b). Statistic comparison was made by 2-way ANOVA followed by Bonferroni test, but no difference was detected.

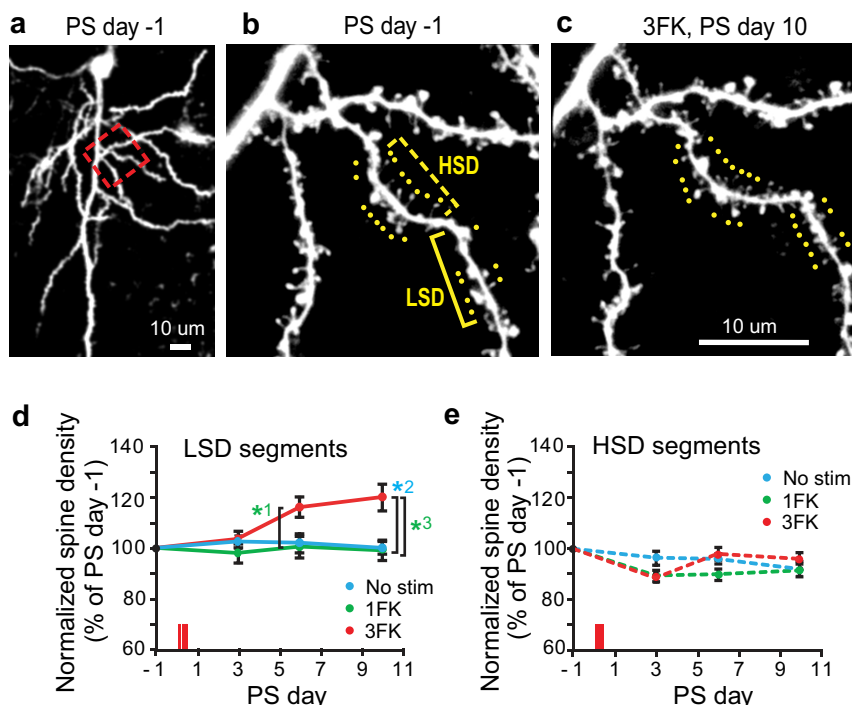


**Figure 4 | Spine density increase classified with respect to pre-existing spine density.** (a) Images (Z-stacked) of a representative cell viewed under a low power. (b, c) High power images of the boxed area in (a) obtained at PS day  $-1$  and PS day 10. Brackets enclose examples of dendritic segments with high and low pre-existing spine densities (referred to as HSD and LSD, respectively). Yellow dots beside the segments indicate spines scored. (d, e) Average spine density changes in LSD and HSD dendritic segments. The numbers of LSD dendritic segments examined are 28, 23, and 31, for No stim, 1FK and 3FK specimens, respectively. The number of HSD segments examined are 16, 16 and 20, for No stim, 1FK and 3FK specimens, respectively. Statistic comparison was made by 2-way ANOVA followed by Bonferroni's test.  $P$  values are 0.043 for \*1, 0.018 for \*2 and 0.016 for \*3.

We examined the fate of pre-existing spines. The stability of pre-existing spines decreased after 3 inductions of LTP (Fig. 6). This may correspond to a recent finding that synaptic activity decreases spine stability<sup>23</sup>. But the stability of spines was different between LSD and HSD segments; spines in LSD segments were more unstable. Medium renewal only (No stim) or the single induction of LTP (1FK) caused no change in spine stability either in LSD or HSD segments.

Our conclusion that the net increase in spine number is preceded by a phase in which the rates of both spine generation and retraction are elevated may be criticized as that imaging intervals adopted would be so large that the periods generation and retraction might not be resolved. Thus we chased individual spines at 1-day intervals, at the sacrifice of the whole period of observation (long observation with short intervals must be avoided for fear of photodynamic damages). As shown in Fig. 7, the rate of spine generation increased continuously until PS day 5, while that of retraction peaked at PS day 2–3, confirming that a period of increased generation and retraction does exist.

To know whether or not the spine number increase proceeds automatically once it is triggered irrespectively to the neuronal activity, we applied tetrodotoxin (TTX) to block spontaneous activity at PS day 4–5 (for 24 h). As shown Fig. 8, the spine number increase was prohibited, suggesting that the spontaneous activity of neurons is necessary for the development of RISE.

## Discussion

To the questions we addressed here, answers are: 1) the dendritic spines increases in number following two phases; the first phase with increased rates of both generation and retraction followed by the second with earlier cessation of spine retraction; 2) the apparent latent period corresponds to the first phase where no net increase

in synapse number is resulted yet; 3) the spine dynamics markedly depends on the pre-existing spine density in the vicinity.

Elevated fluctuation was reported to occur immediately after single induction of electrical LTP<sup>23</sup>. In the present study, however, elevated fluctuation was not significant after single induction of chemical LTP. This discrepancy may be derived from difference in the means of LTP induction, not only electrical versus chemical, but local versus global. Due to the nature of synaptic homeostasis or scaling (the tendency to keep total synapse number of a cell constant)<sup>24</sup>, the drive to increase the synapse number might be lower in the case of global stimulation. Nevertheless, the synapse number is increased by repeated inductions of LTP.

The molecular mechanisms underlying the elevated fluctuation followed by earlier cessation of retraction are undetermined. Since spine dynamics is coupled directly to cytoskeleton dynamics, time-sequence survey on actin and actin-associated proteins should provide wealth of information<sup>15,25</sup>. For discussion on the upstream mechanisms that regulate those cytoskeletal elements, our result on the necessity of spontaneous activity in the period of transition from the elevated fluctuation phase to the biased fluctuation phase is suggestive (Fig. 8; the inhibition of spontaneous firing by TTX during PS day 4–5 blocked the development of RISE). Calcium entry may be critical, since  $Ca^{2+}$  is known to regulate a variety of cytoskeletal elements.

Criticism may arise what activity of the brain *in vivo* corresponds to that spontaneous activity. Behavioral biological studies report the involvement of theta wave and gamma oscillation in memory formation and retrieval<sup>26,27</sup>. Impairment of sharp wave-ripple interferes with memory-related behavior<sup>28</sup>. One or some of these brain activities can be related to the spine dynamics.

Another notable finding in the present study is that the above-mentioned spine dynamics leading to the net spine increase depends on the density of pre-existing spines in the vicinity. Since RISE is

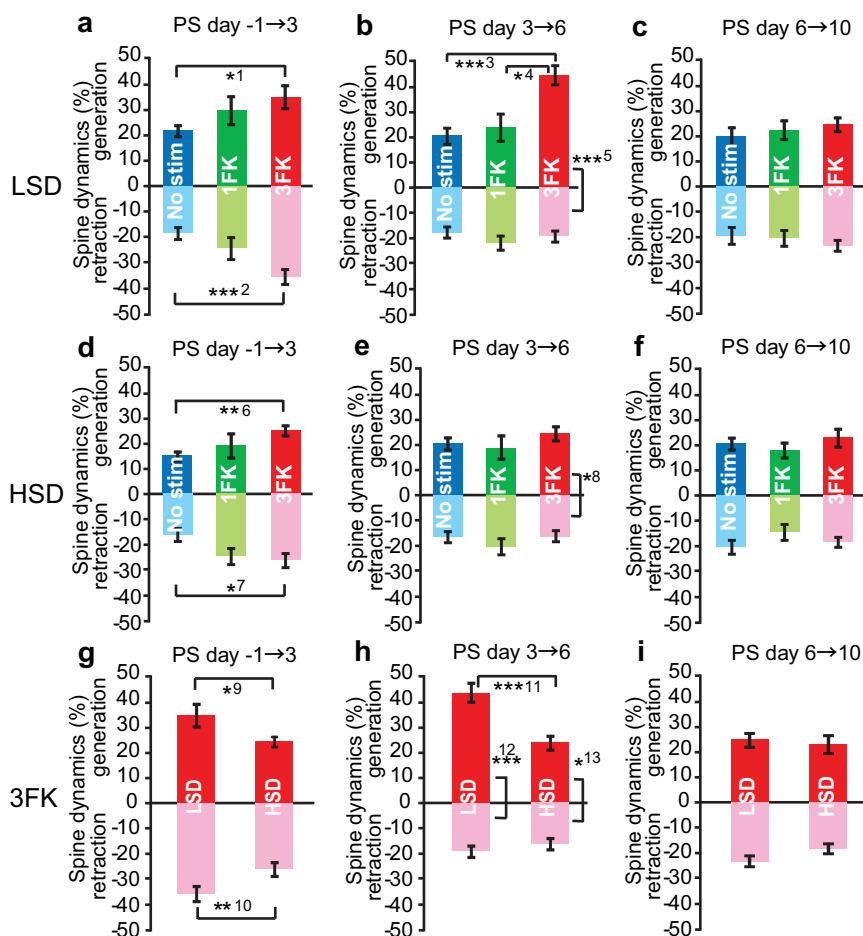


**Figure 5 | Dynamics of individual spines with dendritic segments classified by pre-existing spine density.** (a–c) Dynamics of spines residing on LSD segments. The numbers of segments examined are 14, 11 and 15, for No stim, 1FK and 3FK specimens, respectively. (d–f) Dynamics of spines residing on HSD segments. The numbers of segments examined are 15, 12 and 16, for No stim, 1FK and 3FK specimens, respectively. (g–i) Data re-plotted by matching timings for comparison of LSD and HSD segments. Statistic comparison was made by 2-way ANOVA followed by Bonferroni’s test for comparison among 3 sample groups.  $P$  values are 0.036 for \*1,  $4.4 \times 10^{-4}$  for \*\*\*,  $1.9 \times 10^{-4}$  for \*\*\*, 0.011 for \*4, 0.0029 for \*\*6 and 0.040 for \*7. Statistic comparison between 2 sample groups was made by paired  $t$ -test.  $P$  values are  $4.9 \times 10^{-6}$  for \*\*\*5 (and \*\*\*12), 0.034 for \*8 (and \*13), 0.011 for \*9, 0.0081 for \*\*10 and  $8.5 \times 10^{-5}$  for \*\*\*11.

produced by repetitive inductions of LTP, it is possible that the dependency of RISE on pre-existing spine density would be due to the dependency of LTP *per se* on pre-existing spine density. However, our preliminary examination reveals no such dependency in LTP (see Supplementary Fig. S2 on line; LTP, in which LTP, monitored by an immediate enlargement of spine size, occurred irrespectively to the pre-existing spine density in the vicinity).

The classification of existing spine density to high and low is arbitrary. When we plotted the net spine density increase (spine density at PS day 10 minus that at PS day -1) as a function of spine number at PS day -1, the dependency was not dichotomous but gradual (see Supplementary Fig. S3 on line). For simplicity, however, we use the dichotomous classification to high and low in this report.

The border we set to classify the spine density was 1.3 spines/ $\mu\text{m}$ , the mean spine density in the present cultures. But when we probatively measured the mean dendritic spine density of CA1 pyramidal neurons from the Thy1-YFP H line mice *in vivo*, it was  $\sim 1.4$  spines/ $\mu\text{m}$  for both young (3 weeks) and mature (3 months) individuals (see Supplementary Fig. S4 on line), which was quite similar to the value we obtained in culture. This suggests the existence of an intrinsic limit of spine density.

Since high activity induces spinogenesis, a segment with high spine density should mean that the segment experienced high

activity in past times. Then, would there be saturation of memory, like a fully-written compact disc? In this context, a process for reducing synaptic density becomes important. We reported previously that the repeated inductions of LTD instead of LTP lead to a long-lasting lowering of synaptic strength coupled with synapse elimination, a phenomenon distinct from single LTD<sup>29–31</sup>. It is of interest whether this elimination would occur preferentially in high spine density segments.

The dependency of spine formation on existing spine density should mean that structural synaptic plasticity is regulated not on the basis of individual spines but on the basis of dendritic segments. This theory of “clustered synaptogenesis”<sup>16</sup> emerging recently is often discussed in relation to the convergence of input fibers onto vicinal dendritic loci<sup>17</sup>. In the present study, however, synapses are stimulated globally, nevertheless spines are formed inhomogeneously. This may suggest that the clustered synaptogenesis would be independent of input convergence but regulated by other factors, such as a limited supply of materials for spine growth.

## Methods

**Organotypic slice culture of the mouse hippocampus.** Organotypic slice cultures of the hippocampus were prepared from Thy1-YFP H line mice<sup>32</sup>. The mice (listed as B6.Cg-Tg(Thy1-YFP)Hrs/J; stock number 003782 in the supplier’s catalog) were purchased from The Jackson Laboratory (Maine). The procedures for preparing the

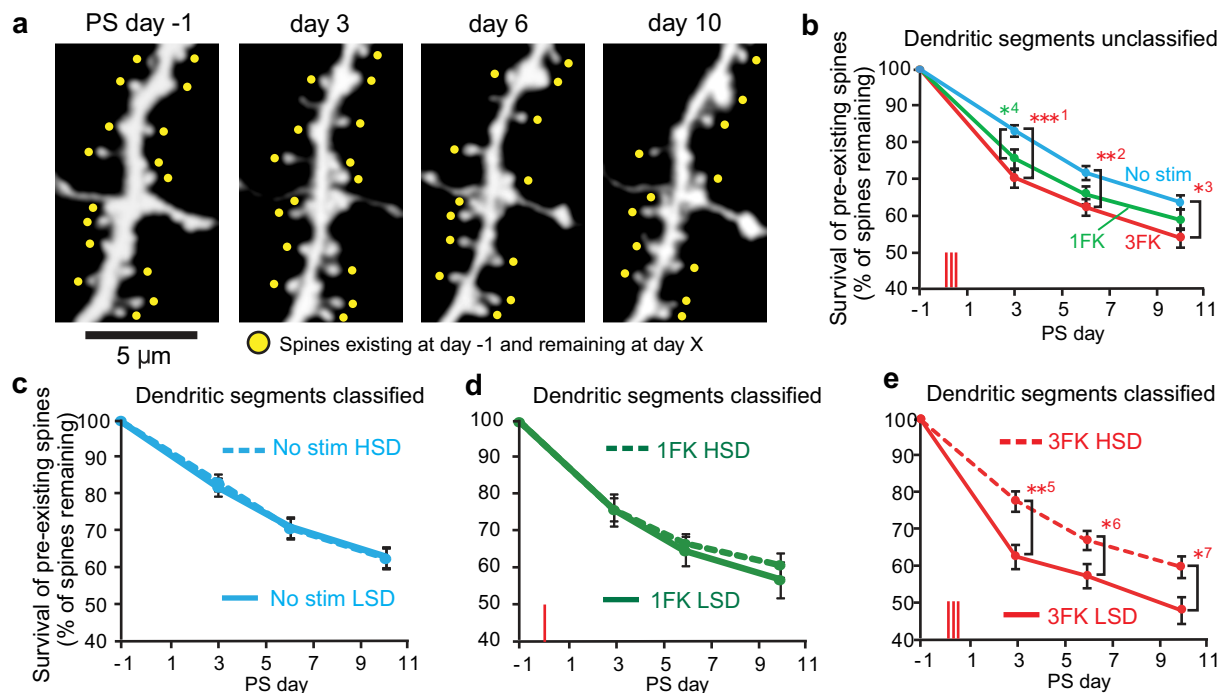


**Figure 6 | Difference in spine survival in LSD and HSD segments.** (a) An example dendritic segment showing the protocol of spine chasing. Yellow dots are the spines that are present in the image of PS day  $-1$  and remaining in the following days. (b) The survival rates of spines with stimulation protocols classified but spine densities unclassified. (c–e) The survival rates of spines with spine densities classified into high (HSD) and low (LSD). In (b–e), the numbers of dendritic segments examined are 30, 32 and 42, for No stim, 1FK and 3FK specimens, respectively. Statistical comparison was made by 2-way ANOVA followed by Bonferroni's test for each time point.  $P$  values are  $2.3 \times 10^{-4}$  for \*\*\*1, 0.0067 for \*\*2, 0.011 for \*3, 0.044 for \*4, 0.0016 for \*\*5, 0.027 for \*6 and 0.021 for \*7.

cultures are the same as previously reported except for the thickness of slices<sup>10</sup>. Briefly, a newborn pup of either sex was anesthetized and sacrificed at postnatal 6–8 days. The hippocampus of either side was isolated and its dorso-ventrally central 1/3 portion was cut into slices with a McIlwain tissue chopper. For electrophysiological examinations, slices were made at 350  $\mu\text{m}$  thickness. For morphological examinations, slices of 250  $\mu\text{m}$  thickness were made to minimize overlapping images of multiple dendrites. Each slice was laid on a piece of polytetrafluoroethylene (PTFE) filter ( $\sim 5 \times 5$  mm), which was placed in an insert of Millicell CF (Millipore) multiwell dish. The cultures were maintained in a fully humidified atmosphere of 34°C for 14–16 days for maturation before beginning experiments<sup>33</sup>. Culture medium, composed of 50% minimal essential medium of Hanks' salt, 25% Hanks' basal salt solution (HBSS) and 25% heat-inactivated horse serum (all from Gibco), was renewed every 3–4 days. The study was carried out in accordance with the Regulation on Animal Experiments of the Animal Experiments Committee of Osaka University. The protocol was approved by the Committee for Animal Experiments of the Osaka University Graduate School of Frontier Biosciences (No. 07-032).

**Chemical LTP induction.** To achieve long-term maintenance of aseptic conditions, LTP was induced by chemical means. Forskolin (FK, Santa Cruz), an adenyl cyclase activator and thus an L-LTP inducer, was dissolved in dimethylsulfoxide at 2 mmol/L for storage. For LTP induction, the slice culture 14–16 days *in vitro* (DIV) was exposed to HBSS containing 20  $\mu\text{M}$  FK (prepared immediately before use). 20 min later, new culture medium was introduced to dilute FK. 340 min later, the second chemical LTP was induced in the same manner and the third chemical LTP was induced another 340 min later (stimulation procedures took 12 h in total). The culture was maintained as before (this specimen is referred to as 3FK). Control specimens were prepared either by limiting the chemical LTP only once (referred to as "1FK") or by medium renewal alone (referred to as "No stim"). The timeline of experiment is diagrammatically shown in Fig. 1a. All manipulations were done at 34°C.

**Electrophysiology.** Extracellular recording of CA1 neuron activity was performed conventionally<sup>10</sup>. Briefly, slice cultures at 14–15 DIV were transferred to a recording chamber and a glass microelectrode filled with ACSF (input resistance, 5–10 M $\Omega$ ) was inserted into the CA1 pyramidal cell layer for recording and a monopolar electrode was placed to the CA3 cell layer for stimulation. Test stimulation pulses of 100  $\mu\text{s}$  duration were delivered every 30 seconds to record field EPSP amplitude. Data were binned for 4 min and plotted.

The protocols for whole cell clamp recording were standard ones<sup>11</sup>. The recording was applied to the neurons of CA1 (recording was not necessarily made from a fluorescing cell). Pipette's inner solution consisted of [mM] 140 CsCl, 1 MgCl<sub>2</sub>, 2 Na<sub>2</sub>ATP, 10 HEPES, 10 EGTA buffered by CsOH at pH 7.2. To monitor miniature

excitatory synaptic current (mEPSC), artificial cerebrospinal fluid (ACSF) containing 1  $\mu\text{M}$  tetrodotoxin (TTX, Alomone), 25  $\mu\text{M}$  aminophosphonovalerate (Tocris) and 10  $\mu\text{M}$  bicuculine methiodide (Wako) was perfused. By clamping the membrane potential at  $-60$  mV, collected current was fed to a MultiClamp 700A (Axon Instruments) amplifier, with digitization at 10 kHz and low-pass filtering at 2 kHz. The threshold for mEPSC detection was set at 3 pA. The amplitude and the frequency of mEPSC were analyzed from 100 events randomly selected from each neuron using Clampfit software (Molecular Devices). The slice served for electrophysiology was not returned to culture. Hence, the data shown in Fig. 3 were obtained from separate slices. To minimize influence from the peculiarity of individual slices, the number of cells recorded from a single slice was three or less.

**Microscopic morphometry.** Laser confocal microscopy was applied to the first branch (emerging from the dendritic shaft) or the second branch (emerging from the first branch) of the apical dendrites of the CA1 pyramidal cells located within 1001  $\mu\text{m}$  from the soma. To minimize the effect of culture medium exchange on spine dynamics, we fixed the timing of medium renewal at 3 days prior to observation. For long-term imaging, the first observation was performed one day before repeated FK applications (referred to as poststimulus [PS] day  $-1$ ), the second observation at 3 days (referred to as PS day 3), the third at 6 days (PS day 6), and the final at 10 days after 3 FK-exposures (PS day 10). In case of examinations at 1-day intervals, however, no medium renewal was done up to PS day 5 for fear that the extremely frequent medium renewal would perturb the cells' viability.

A laser-scanning confocal optics (Olympus FV300; single photon system) was mounted onto an Olympus IX71 inverted epifluorescence microscope equipped with a 60 $\times$  water immersion objective lens (UplanSApo60, NA 1.20). On a thermostated stage (Tokai-hit, set at 34°C), a glass-bottom dish (Matsunami) was placed, within which the filter piece carrying a cultured slice was laid. 50  $\mu\text{l}$  aliquot of the original culture medium was transferred onto the top of the slice to prevent drying and no medium perfusion was made during image acquisition. To avoid photobleaching of fluorescence, laser intensity was limited to 1–3% of maximum. Acquisition conditions were unchanged over different days of observation. In this optics system, 1  $\mu\text{m}$  in the X-Y plane corresponds to 17 pixels, and the image size for long term spine observation was 60  $\mu\text{m} \times 60 \mu\text{m}$ . A YFP-positive pyramidal neuron sitting approximately in the center of CA1 *stratum pyramidale* was selected to acquire serial images at 0.75  $\mu\text{m}$  Z-axis steps. After first imaging (PS day  $-1$ ), a low magnified image was acquired and stacked into a two-dimensional plane for the aid of identifying the target cell in later examinations. In the cultures of 250  $\mu\text{m}$  thickness, the tendency of flat dendritic arborization was prominent so that not many of the first and second dendritic branches ran obliquely in the Z-axis direction. Nevertheless, to minimize errors in spine density, we chose dendritic segments running for more than

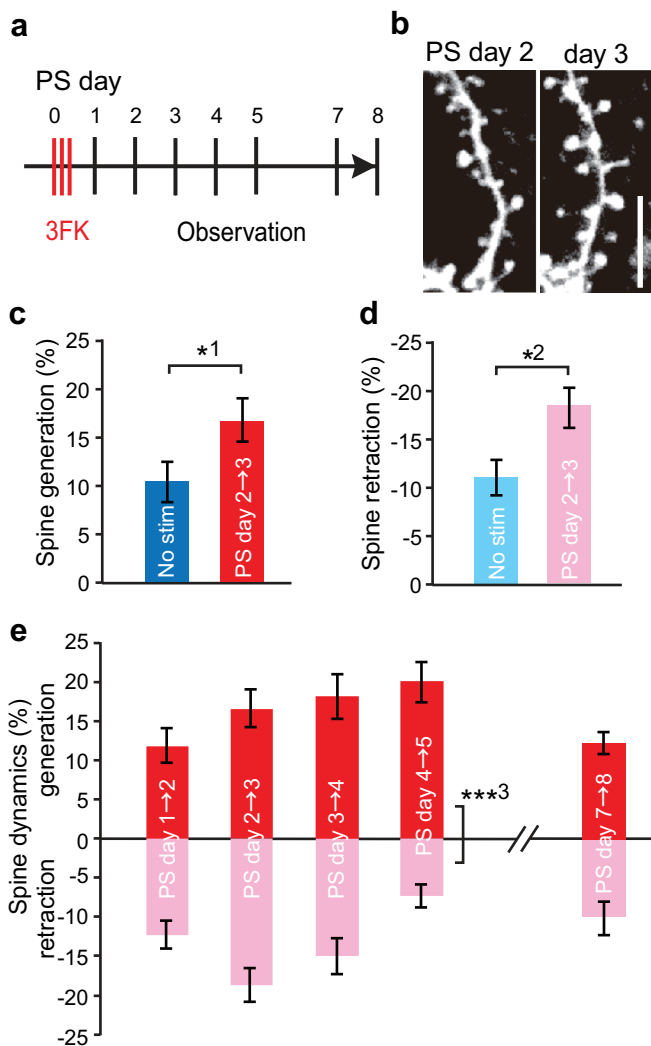


**Figure 7 | Spine dynamics as monitored at 1-day intervals after 3 LTP inductions.** (a) Timeline of experimental procedures. (b) Representative images of a dendrite. Scale bar indicates 5  $\mu\text{m}$ . (c, d) Rates of spine generation and retraction per day at the timing of PS day 2–3 as compared with those of unstimulated specimens (paired  $t$ -test). The numbers of dendritic spines (LSD only) examined are 18 (No stim) and 25 (Stimulated).  $P$  values are 0.045 for \*1 and 0.011 for \*2. (e) Comparisons between the rates of spine generation and retraction per day. The absolute values do not coincide with those in Fig. 2, since some proportion of spines are generated and retracted quickly within the scoring intervals. The number of segments (LSD only) examined are 21, 25, 24 and 27 and 9, for PS day1–2, PS day2–3, PS day3–4, PS day4–5 and PS day 7–8 specimens, respectively. Statistic comparison, by paired  $t$ -test, was applied between generation and retraction.  $P$  value is  $1.5 \times 10^{-4}$  for \*\*\*3.

~10  $\mu\text{m}$  horizontally within three focal planes (central focal plane plus 1 step up and down the Z-axis).

Analyses were performed on an imageJ software, the number of spines was counted by a cell counter plugin and the length of dendrite was measured by segmented line tool from a raw picture under blind conditions. By comparing two images, a spine recognized in the present image but not in the previous one was referred to as “generated” and a spine recognized in the previous image but not in the present one was referred to as “retracted”. A spine displaced laterally within 0.7  $\mu\text{m}$  in appearance was judged identical. Although filopodia were rare in our preparation (probably because of well matured culture), we excluded filopodium-like protrusions from counting following conventional criteria<sup>21</sup>: head diameter  $\leq 1.2 \times$  neck diameter or neck length  $\geq 3 \times$  neck diameter. The rates of spine generation and retraction were represented as percentages to total the spine number in the segment under examination. Spine stability was determined by chasing the spines existing at PS day –1 and presented as percentage of remaining spines. The number of cells for monitoring

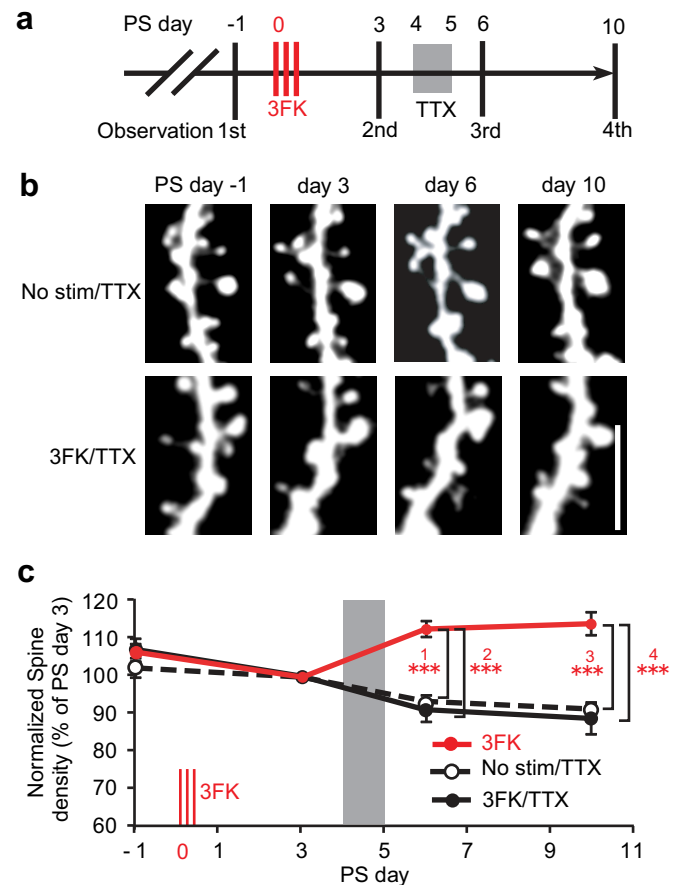


**Figure 8 | Requirement of spontaneous activity for the development of RISE.** (a) Timeline of experimental procedures. Tetrodotoxin (TTX; 1  $\mu\text{M}$ ) was applied during the period indicated in gray to both No stim and 3FK specimens. (b) Time-sequenced images of representative dendritic segments. Scale bar indicates 5  $\mu\text{m}$ . (c) TTX suppressed the increase in spine density. This result serves also as collateral evidence for the formation of functional synapses on the newly generated spines. The number of dendritic segments examined are 9 and 9, for No stim/TTX and 3FK/TTX samples, respectively. The data for 3FK are cited from Fig. 1d (ratios were re-calculated). Statistic comparison was made by 2-way ANOVA followed by Bonferroni’s test for each time point.  $P$  values are  $8.8 \times 10^{-4}$  for \*\*\*1,  $4.4 \times 10^{-5}$  for \*\*\*2,  $5.2 \times 10^{-4}$  for \*\*\*3 and  $4.3 \times 10^{-5}$  for \*\*\*4.

in a single slice was less than 2. In total, we analyzed 22 slices for 3FK, 14 slices for 1FK, 14 slices for No stim, 13 slices for No stim/TTX, and 12 slices for 3FK/TTX. The number of spines chased in present study was 52119. Imaging procedures were completed within 30 min before the slice was returned to the original Millicell filter insert to continue culturing.

**Statistic analysis.** In all figures which include statistic comparisons, means  $\pm$  standard errors of means are indicated. The number of specimens examined is indicated within each figure legend. For the comparison of two sample groups, a Welch’s paired  $t$ -test assuming non-identical variance was applied. For the comparison of  $\geq 3$  sample groups, ANOVA followed by Bonferroni’s test was applied. For the comparison of cumulative histograms, a Smirnov-Kormogorov test was applied. Statistically significant differences are shown as \* (for  $P < 0.05$ ), \*\* (for  $P < 0.01$ ), or \*\*\* (for  $P < 0.001$ ). Regression analysis was applied in case of necessity. Exact  $P$  values are indicated in the figures or figure legends.

- Ebbinghaus, H. *Über das Gedächtnis*. 1885. Translated in English as *Memory: A Contribution to Experimental Psychology*. (Columbia Univ. 1913).
- Pavlov, I. P. *Lektsii o Rabote Bolshih Polusharij Golovnogo Mozga*. 1927. Translated in English as *Conditioned Reflexes: An Investigation of the Physiological Activity of the Cerebral Cortex* (Oxford Univ. Press 1927).
- Frost, W. N., Castellucci, V. F., Hawkins, R. D. & Kandel, E. R. Monosynaptic connections made by the sensory neurons of the gill- and siphon-withdrawal reflex in *Aplysia* participate in the storage of long-term memory for sensitization. *Proc. Natl Acad. Sci. USA* **82**, 8266–8269 (1985).



4. Bernabeu, R. *et al.* Involvement of hippocampal cAMP/cAMP-dependent protein kinase signaling pathways in a late memory consolidation phase of aversively motivated learning in rats. *Proc. Natl Acad. Sci. USA* **94**, 7041–7046 (1997).
5. Bekinschtein, P. *et al.* Persistence of long-term memory storage requires a late protein synthesis- and BDNF-dependent phase in the hippocampus. *Neuron* **53**, 261–277 (2007).
6. Eckel-Mahan, K. L. *et al.* Circadian oscillation of hippocampal MAPK activity and cAMP: implications for memory persistence. *Nature Neurosci.* **11**, 1074–1082 (2008).
7. Schwartzkroin, P. A. & Wester, K. Long-lasting facilitation of a synaptic potential following tetanization in the *in vitro* hippocampal slice. *Brain Res.* **89**, 107–119 (1975).
8. Malenka, R. C. & Bear, M. F. LTP and LTD: An embarrassment of riches. *Neuron* **44**, 5–21 (2004).
9. Stoppini, L., Buchs, P. A. & Muller, D. A simple method for organotypic cultures of nervous tissue. *J. Neurosci. Meth.* **37**, 173–182 (1991).
10. Tominaga-Yoshino, K., Kondo, S., Tamotsu, S. & Ogura, A. Repetitive activation of protein kinase A induces slow and persistent potentiation associated with synaptogenesis in cultured hippocampus. *Neurosci. Res.* **44**, 357–367 (2002).
11. Tominaga-Yoshino, K., Urakubo, T., Okada, M., Matsuda, H. & Ogura, A. Repetitive induction of late-phase LTP produces long-lasting synaptic enhancement accompanied by synaptogenesis in cultured hippocampal slices. *Hippocampus* **18**, 281–293 (2008).
12. Urakubo, T., Tominaga-Yoshino, K. & Ogura, A. Ultrastructural features of hippocampal CA1 synapses with respect to synaptic enhancement following repeated PKA activation. *Neurosci. Lett.* **407**, 1–5 (2006).
13. Kawaai, K. *et al.* Analysis of gene expression changes associated with long-lasting synaptic enhancement in hippocampal slice cultures after repetitive exposures to glutamate. *J. Neurosci. Res.* **88**, 2911–2922 (2010).
14. Oe, Y., Tominaga-Yoshino, K. & Ogura, A. Local establishment of repetitive long-term potentiation-induced synaptic enhancement in cultured hippocampal slices with divided input pathways. *J. Neurosci. Res.* **89**, 1419–1430 (2011).
15. Yasumasu, N., Matsuzaki, M., Miyazaki, T., Noguchi, J. & Kasai, H. Principles of long-term dynamics of dendritic spines. *J. Neurosci.* **28**, 13592–13608 (2008).
16. Losonczy, A., Makara, J. K. & Magee, J. C. Compartmentalized dendritic plasticity and input feature storage in neurons. *Nature* **452**, 436–441 (2008).
17. Takahashi, N. *et al.* Locally synchronized synaptic inputs. *Science* **335**, 353–356 (2012).
18. Fu, M., Yu, X., Lu, J. & Zuo, Y. Repetitive motor learning induces coordinated formation of clustered dendritic spines *in vivo*. *Nature* **483**, 92–95 (2012).
19. Zuo, Y., Lin, A., Chang, P. & Gan, W. B. Development of long-term dendritic spine stability in diverse regions of cerebral cortex. *Neuron* **46**, 181–189 (2005).
20. Xu, T. *et al.* Rapid formation and selective stabilization of synapses for enduring motor memories. *Nature* **462**, 915–919 (2009).
21. Yang, G., Pan, F. & Gan, W. Stably maintained dendritic spines are associated with lifelong memories. *Nature* **462**, 920–924 (2009).
22. Zito, K., Scheuss, V., Knott, G., Hill, T. & Svoboda, K. Rapid functional maturation of nascent dendritic spines. *Neuron* **29**, 247–258 (2009).
23. De Roo, M., Klausner, P. & Muller, D. LTP promotes a selective long-term stabilization and clustering of dendritic spines. *PLoS Biol.* **6**, e219 (2008).
24. Turrigiano, G. G. The self-tuning neuron: synaptic scaling of excitatory synapses. *Cell* **135**, 422–435 (2008).
25. Rex, C. S. *et al.* Different Rho GTPase-dependent signaling pathways initiate sequential steps in the consolidation of long-term potentiation. *J. Cell. Biol.* **186**, 85–97 (2009).
26. Rutishauser, U., Ross, I. B., Mamelak, A. N. & Schuman, E. M. Human memory strength is predicted by theta-frequency phase-locking of single neurons. *Nature* **464**, 903–907 (2010).
27. Carr, M. F., Karlsson, M. P. & Frank, L. M. Transient slow gamma synchrony underlies hippocampal memory replay. *Neuron* **75**, 700–713 (2012).
28. Girardeau, G., Benchenane, K., Wiener, S. I., Buzsáki, G. & Zugaro, M. B. Selective suppression of hippocampal ripples impairs spatial memory. *Nature Neurosci.* **12**, 1222–1223 (2009).
29. Shinoda, Y., Kamikubo, Y., Egashira, Y., Tominaga-Yoshino, K. & Ogura, A. Repetition of mGluR-dependent LTD causes slowly developing persistent reduction in synaptic strength accompanied by synapse elimination. *Brain Res* **1042**, 99–107 (2005).
30. Kamikubo, Y. *et al.* Long-lasting synaptic loss after repeated induction of LTD: independence to the means of LTD induction. *Eur. J. Neurosci.* **24**, 1606–1616 (2006).
31. Egashira, Y. *et al.* Involvement of the p75<sup>NTR</sup> signaling pathway in persistent synaptic suppression coupled with synapse elimination following repeated long-term depression induction. *J. Neurosci. Res.* **88**, 3433–3446 (2010).
32. Feng, G. *et al.* Imaging neuronal subsets in transgenic mice expressing multiple spectral variants of GFP. *Neuron* **28**, 41–51 (2000).
33. Muller, D., Buchs, P. A. & Stoppini, L. Time course of synaptic development in hippocampal organotypic cultures. *Brain Res. Dev. Brain Res.* **71**, 93–100 (1993).

## Acknowledgments

This study was supported by funds from the Japanese Ministry of Education, Culture, Sports, Science and Technology to A. O. (23300132 and 24650207).

## Author contributions

K.T.-Y. and A.O. designed research; Y.O. and S.H. performed research (morphometry); K.T.-Y. performed research (electrophysiology); and A.O. wrote the paper.

## Additional information

**Supplementary information** accompanies this paper at <http://www.nature.com/scientificreports>

**Competing financial interests:** The authors declare no competing financial interests.

**License:** This work is licensed under a Creative Commons Attribution-NonCommercial-NoDerivs 3.0 Unported License. To view a copy of this license, visit <http://creativecommons.org/licenses/by-nc-nd/3.0/>

**How to cite this article:** Oe, Y., Tominaga-Yoshino, K., Hasegawa, S. & Ogura, A. Dendritic spine dynamics in synaptogenesis after repeated LTP inductions: Dependence on pre-existing spine density. *Sci. Rep.* **3**, 1957; DOI:10.1038/srep01957 (2013).